Tradeoff-mediated Drought Legacy in Soil Microbiome

Abstract

The irreplaceable, profound role of soil microbiome in completing biogeochemical cycling in the Earth System renders pivotal understanding its response to drought of increasing frequency and severity toward evaluating drought-mediated biosphere-atmosphere interactions. Though with over a-half century of extensive research on drought impacts on soil microbiomes, drought legacy, a phenomenon of persistence (or memory) of past disturbance that has been widely discussed in soil microbiome (and broadly across natural systems) and may largely influence microbiome and ecosystem functioning, is still with a yet unresolved explicit mechanism. Here, using a trait-based microbial systems modelling framework with an explicit intra-cellular metabolic allocation of enzyme, osmolyte, and thus emergent yield, we revealed a range of representative drought legacy scenarios from persistent through transient to no legacy at all depending on drought intensity and microbial dispersal. Emerging from the tradeoff between enzyme investment and drought tolerance at both the physiological and community level, these legacy scenarios can be organized into a coherent mechanistic framework based on Y(Yield)-A(Acquisition)-S(Stress). Any factor or process that can influence the physiological tradeoff between resource acquisition (i.e., enzymes) and stress tolerance (e.g., osmolytes) and change the trajectory of a community on the YAS constrained space would alter the property of drought legacy. This overarching mechanistic insight into soil microbiome drought legacy hold tremendous promise to more accurately quantifying soil microbiome resilience and functioning. Meanwhile, this study inspires us to couple microbiome with vegetation with a holistic ecosystem view by capturing major tradeoff dimensions to evaluate drought-biosphere interactions.

1 Introduction

Drought of increasing severity and frequency both regionally and worldwide is one of the most pressing problems to the biosphere (e.g., **Borsa et al. 2014; Berdugo et al. 2020**). The unparalleled role of soil microbiome in driving materials' cycling in the Earth system (**Falkowski et al. 2008**) makes incorporating its response to drought integral for systematically evaluating drought impacts on the biosphere, which, however, is still largely missing or implicitly treated in global assessments of drought-biosphere interactions (e.g., **Green et al. 2019**). Over a-half century of research has uncovered a myriad of physio-chemical, physiological, and ecological mechanisms underlying immediate microbial systems functional changes to drought disturbance in soil environment (e.g., **Birch 1958; Schimel 2007; Manzoni et al. 2012**). However, persistence of the past drought perturbation-induced changes in soil microbiome (e.g., **Evans and Wallenstein 2012**; **Meisner et al. 2015**; **Hawkes et al. 2017; Martiny et al. 2017; Hinojosa et al. 2019**), a phenomenon termed drought legacy that has also been widely observed across the forest biome and beyond (e.g., **Anderegg et al. 2015; Johnstone et al. 2016; Conradi et al. 2020**), still misses a compelling mechanistic explanation. Legacy determines resilience; elucidating the occurrence of soil microbiome drought legacy is indispensable for understanding microbial systems resilience. A better understanding of legacy and resilience can draw a complete picture of soil microbiome functioning constrained by both contemporary and historical drought conditions, which will be essential immediately for more accurately quantifying organic matter decomposition and eventually for quantifying responses and feedbacks of whole ecosystems to drought in the Earth System.

Intuitively, formation of legacy originates from persistence of microbial systems changes after a drought disturbance. Microbial systems are complex adaptive systems, with their

functioning emerging from tremendous individual variation and within-community interactions. Past lab- and field-based efforts successfully explained soil microbiome drought legacy by proposing to depict compositional differences in terms of a few functional types of different life-history strategies. Notably, **Hawkes and Keitt (2015)** proposed a mechanism of community shift in relative abundance of moisture generalist vs. specialist, of which generalist is functionally more stable than specialists with moisture. This idea was argued to explain the observation of a lack of change in moisture response across sites in Texas, USA because of observed dominance by generalist taxa resulting from high variation in historical rainfall (**Hawkes et al. 2017; Waring and Hawkes 2018**). Similarly, **Evans and Wallenstein** (**2014**) argued soils with relatively stable moisture history had more moisture-sensitive taxa and hence larger changes in biomass and composition (**Evans and Wallenstein 2012**). However, a major deficiency of these pioneering coarse functional group-based community shifts is that they lack an explicit underlying physiological basis, which cannot really tell how a microbial community can be really shaped by drought disturbance from the bottom up and how its functional change can persist. This deficiency becomes especially apparent when having many studies at different sites with varying confounding factors reporting legacies of varying magnitudes with differing time frames, especially those that even did not observe a drought legacy at all (e.g., **Rousk et al. 2013; Fuchslueger et al. 2016**). In fact, such a missing of mechanistic details also applies to warming-induced legacy in microbial systems functioning (e.g., **Karhu et al. 2014**). We need to link individual-level physiological variation to community-level shift to explain persistence of microbial systems functioning.

Trait-based quantification of microbial systems complexity can bridge the gap between underlying large physiological variability and community dynamics (e.g., **McGill et al. 2006**). Moreover, a field manipulative experiment at a grassland ecosystem in Southern California

measured drought legacy attributed to bacterial composition change with an alteration of carbohydrate degradation traits but not for nitrogen addition that instead did not present a change in carbohydrate degradation traits (**Martiny et al. 2017**). This clear contrast directly motivates us to find a trait-based linkage between microbial physiology and community shift underlying legacy. Physiologically, it is well established that a microbial cell can direct available resources from producing exoenzymes to acquire resources to produce compounds, e.g., osmolytes, to combat desiccation (e.g., **Schimel 2007**), an intra-cellular metabolic plasticity that displays large inter-cellular variability (e.g., **Manzoni et al. 2012**). Quantifying the individual-level metabolic variation in these metabolic processes using physiological traits that reflect and determine demographic variation and tradeoff between individuals, a trait-based mechanistic framework, Y-A-S (Yield-Acquisition-Stress), has been proposed (**Malik et al. 2019**). Based on this framework, against the need to increase community-level drought tolerance to combat drought pressure tradeoff-mediated physiological adaptation and turnover of individuals comprising a microbial community should drive a community to lower its enzyme investment. Thereby, a drought legacy in organic matter decomposition may arise from the persistence of this functional change in terms of enzyme investment. With this reasoning, any factor that can modify such a tradeoff should alter the property, magnitude, and duration of drought legacy. For instance, the intensity of drought, which directly modulates intracellular metabolic allocation (**Csonka 1989; Schimel 2007**), may strongly shape the tradeoff and hence affect legacy. In addition, dispersal of microbes, a pivotal process influencing community composition and dynamics via introducing taxa (e.g., **Fukami 2015; Vila et al. 2019**) that cannot directly affect the individual-level metabolic tradeoff, may instead change the community-level tradeoff emerged and hence alter drought legacy (**Hawkes et**

al. 2017). Therefore, this trait-based tradeoff underlying the YAS framework is supposed to govern drought legacy in soil microbiome.

Theory-driven trait-based modelling is well positioned to transcend limitations embedded in the current generation of lab- and field-based investigations to test this trait-based mechanism underpinning soil microbiome drought legacy. Trait-based modelling in an individual-based framework is able to bridge across scales from individual cell through community to the system level by explicitly simulating intra-cellular metabolic processes, ecological dynamics of microbial communities, and emergent functioning (**Allison 2012**). Such a modelling approach is superior to the prevailing aggregated modelling approach of treating microbes as a single biomass pool or a few discrete functional groups [see a review by **Wieder et al. (2015**)]. In addition, a more direct stimulus of modelling legacy is that it can directly test the claim that including legacy would be trivial in biogeochemical modelling (**Rousk et al. 2013**).

Does the trait-based, tradeoff-mediated mechanism underpin soil microbiome drought legacy? This study addressed this overarching question using a mechanistically and spatially explicit trait- and individual-based soil microbial systems modelling framework—DEMENTpy, built with a central assumption of intra-cellular metabolic plasticity that enables resource acquisition vs. drought tolerance tradeoff. Specifically, these following questions were answered: how does the magnitude of drought legacy in decomposition vary with drought intensity? How does dispersal of microbes affect the formation of drought legacy? What are the underlying changes in traits of enzyme investment and drought tolerance? And finally can these changes be put into a coherent mechanistic framework based on YAS? We tackled these questions by applying the DEMENTpy to a grassland ecosystem in Southern California. This study would open up rich possibilities for trait-based investigations into microbiome legacy and resilience and into

implications of their interactions with vegetation dynamics for the biosphere-atmosphere interactions.

2 Methods

2.1 Model description

DEMENTpy (DEcomposition Model of ENzymatic Traits in Python; GitHub Repository: https://github.com/bioatmosphere/DEMENTpy) is a spatially and mechanistically explicit trait- and individual-based microbial systems modelling framework built upon its predecessor DEMENT (**Allison 2012; Allison and Goulden 2017; Wang and Allison 2019**). This model randomly initializes a microbial community on a spatial grid based on physiological traits and simulates its dynamics by modelling explicitly demographic processes of each population including cell metabolism and growth, mortality, and reproduction at a daily time step. Driven by temperature and moisture, the community secretes different exoenzymes decomposing different organic compounds. Starting from continuous physiological traits, DEMENTpy bridges across scales from individual through community to systems in soil microbiome (see **Supporting Fig. 1** for model structure). Only community initialization and intra-cellular metabolic allocation are highlighted below. More details with respect to structure, processes, formula, and parameters are referred to the **Supporting Information.**

With a trait-based approach, DEMENTpy creates a microbial community composed of a large number of hypothetical taxa by randomly drawing values from uniform distributions of microbial traits and assigning them to different taxa (see a list of traits in **Supporting Fig. 1B** and more details in **Supporting Text**). The traits include rates of enzyme production (constitutive and inducible) and rates of osmolyte production (constitutive and inducible). Drought tolerance of each

taxon is determined by normalizing the inducible osmolyte rate of production to a value from 0 to 1. This formulation establishes a mechanistic connection between osmolyte production and drought tolerance (**Schimel 2007**) in contrast to the previous model version which instead directly introduced a drought tolerance parameter and imposed a penalty on carbon use efficiency accordingly (**Allison and Goulden 2017**).

DEMENTpy explicitly treats intra-cellular metabolism of ingested monomer carbon derived from explicit exoenzymatic degradation of substrates (**Supporting Fig. 1C**; see **Supporting Text** for substrate degradation and other demographic processes). The metabolic processing of assimilated carbon after growth respiration is directed to produce enzyme (and maintenance respiration) and osmolyte (and maintenance respiration; **Csonka 1989; Witteveen and Visser 1995**), which are treated as simultaneous processes without prescribing an order. After accounting for the constitutive production of enzymes and osmolytes, the carbon left after these inducible processes accumulates toward biomass (denoted as yield). We assume the constitutive osmolyte production rate varies across taxa but independent of water potential, accounting for bacterial/fungal cell's allocation of biomass to keep a water potential balance across cell wall (**Csonka 1989**). By contrast, inducible production of osmolytes is subject to constraints from water potential only below a certain threshold. Arising from metabolic production of enzyme and osmolyte and accompanying maintenance and respiration, mortality of microbial cells is simulated both deterministically by accounting for mass balance and stochastically based on death probability constrained by drought tolerance and water potential.

2.2 Modelling experiments

We applied DEMENTpy to the grassland system at Loma Ridge, Southern California (**Allison et al. 2013**) and parameterized the model with 100 different hypothetical bacterial taxa

on a 100 by 100 spatial grid decomposing grass litter containing ten different substrates (see parameter values in **Supporting Table 1** and substrates in **Supporting Table 2**). DEMENTpy was benchmarked with the daily weather data of year 2011, which is treated as the ambient scenario (**Supporting Fig. 2A)**, based on whitch results presented below were robust to reasonably varying the parameter value range of basal enzyme and osmolyte production rate.

On top of this ambient scenario we conducted simulations with manipulated drought to examine drought disturbance to the microbial system with respect to responses and recoveries in three 3 phases (**Supporting Fig. 2**). Two drought scenarios, moderate and severe, were created by reducing the water potential across only the dry season by a factor of four and ten, respectively. After the community establishment phase and a successive drought period, the ambient scenario was re-imposed to examine changes in microbial communities degrading substrates. One set of such simulations without dispersal is referred to as default mode. Another set in dispersal mode with only the ambient and severe drought scenario is set to further examine how dispersal affects drought disturbance over time.

2.3 Simulation protocol and data analysis

With the model setup as above, we conducted three-phase simulations following the protocol as follows (**Supporting Fig. 2**). After establishing an initial microbial community from a randomly constructed microbial pool on the spatial grid with homogeneously distributed substrates, each simulation was run for 10 years at a daily time step (spin-up: 3 years; disturbance: 3 years; recovery: 4 years). In each new year substrates, monomers, and enzymes were reinitialized uniformly on the spatial grid to have the same configurations as the very first year except for the microbial community. In each new year the microbial community on the spatial grid was also randomly reinitialized based on the same microbial pool. Two different methods were applied to

differentiate between the default and dispersal mode: for the default mode, microbial community was determined according to frequency of each taxon on the grid based on their biomass in the very last day of the previous year (**Supporting Fig. 2C**); in the dispersal mode the frequency based on cumulative biomass of each taxon across the previous whole year was applied (**Supporting Fig. 2D**). In contrast to the default mode, cumulative frequency makes possible those dead taxa in the previous year being introduced into the community in the next year, forming a simplistic but effective strategy simulating dispersal. These simulations were repeated for each scenario under the two modes (default and dispersal mode) for 40 times with 40 different seeds ($5 \times 40 = 200$ runs in total). This sample size was determined by a convergence analysis of DEMENTpy's stochastic nature (**Supporting Fig. 3**).

All results presented in this work, unless indicated otherwise, were analyses of such an ensemble of 40 runs for each of the five scenarios. A dataset was established from these simulations encompassing taxon traits (enzyme investment and drought tolerance), time-series of taxon-specific allocation to enzymes(inducible plus constitutive), osmolytes (inducible plus constitutive), yield, and biomass in carbon, and time-series of community-level carbon allocation (enzymes, osmolytes, and yield), as well as time-series of compound-specific and total substrates. Taxon-specific allocation to enzymes, osmolytes, and yield were aggregated to derive the corresponding community-level allocation. With taxon traits and biomass, biomass-weighted community-level traits, enzyme investment and drought tolerance, were calculated (see the **Supporting Text** for calculation method). Because the system largely stabilized in 3 years (**Supporting Fig. 2**), of the 10-yr simulations data at most to the year 9 (3_{rd} year of recovery from drought disturbance) were presented. In addition, 95% confidence intervals were presented in most

of the cases except for microbial community composition and community carbon allocation, for which results of only one out of the 40 simulations were shown.

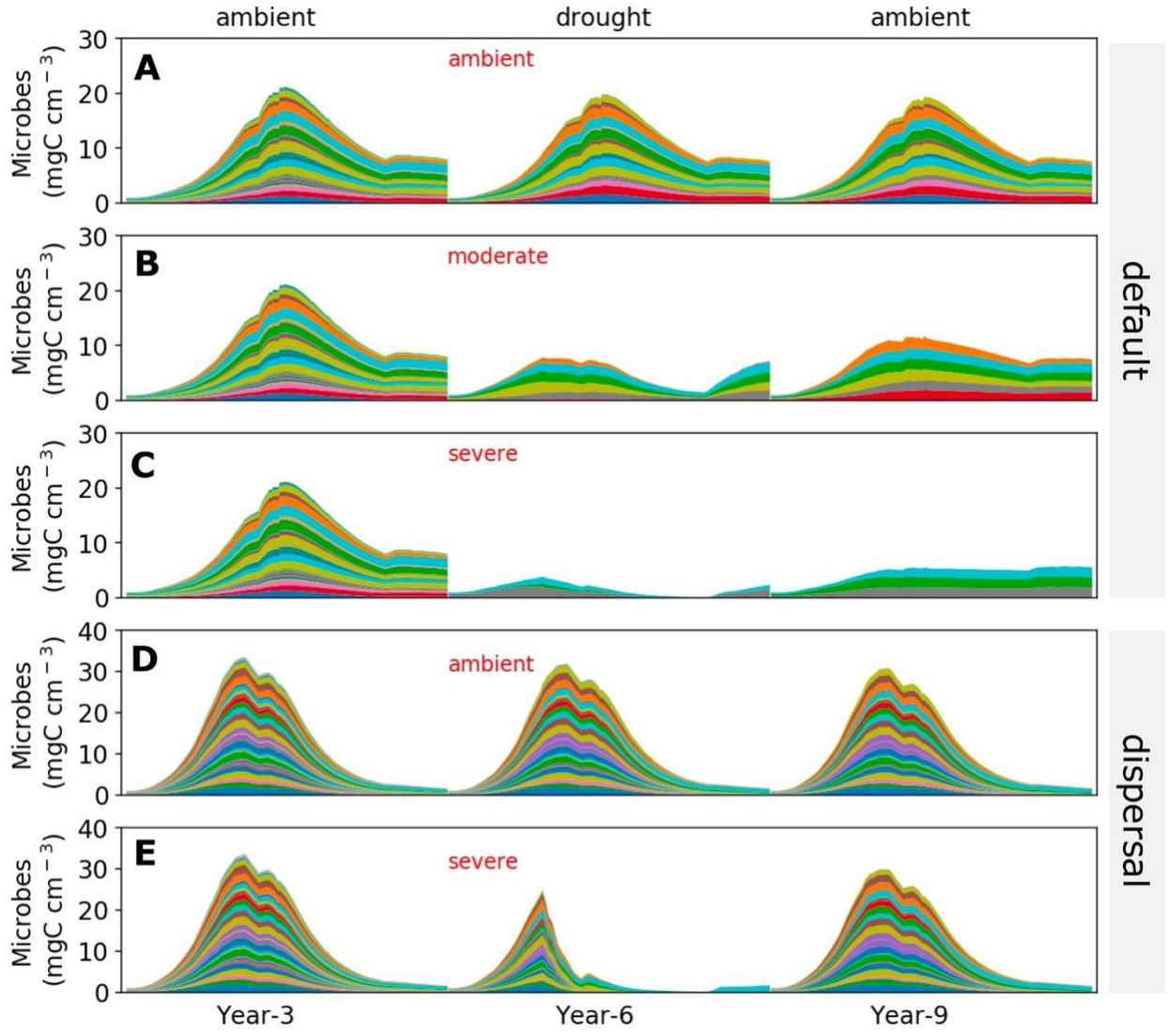

Fig.1. Microbial community dynamics disturbed by drought of differing severities with and without dispersal. (**A-C**) Dynamics without dispersal under ambient, moderate, and severe scenario, respectively. (**D, E**) Dynamics with dispersal under ambient and severe scenario, respectively. Colored bands represent different hypothetical taxa in terms of biomass (mg C cm^{-3}) averaged over the 100×100 spatial grid. Data shown are only for years 3, 6 (the 3rd year under

drought), and 9 (the 3rd year after drought). See **Supporting Fig. 2** for the full 10-year dynamics under the ambient scenario of both default and dispersal mode.

3 Results

3.1 Microbial community dynamics under the ambient drought scenario

The system became relatively stable after 2 years, with seasonal dynamics in the microbial community repeating across years (**Supporting Fig. 2**). Seasonal dynamics with respect to community composition and biomass reflected a joint control by environment and substrates. Starting from the wet season that was replete with substrates, a microbial community consisting of different taxa established and grew in biomass. As substrates were degraded and depleted, microbial cells began to starve and die. Increasing drought while entering the dry season induced more death. These two processes in combination resulted in the decline of microbial biomass after a biomass peak around 20 mg C cm^{-3} (**Fig. 1A)** and drove the composition toward taxa with higher drought tolerance and lower enzyme investment (**Supporting Fig. 4A**) and hence community level enzyme investment decrease (**Fig. 2A**) and drought tolerance increase across the dry season (**Fig. 2B**). Similar seasonal and inter-annual dynamics were observed for the community with dispersal but with much higher biomass (peaked around 30 mg C cm^{-3}) and taxonomic diversity (**Fig. 1D; Supporting Fig. 4B; Fig. 2C, D**).

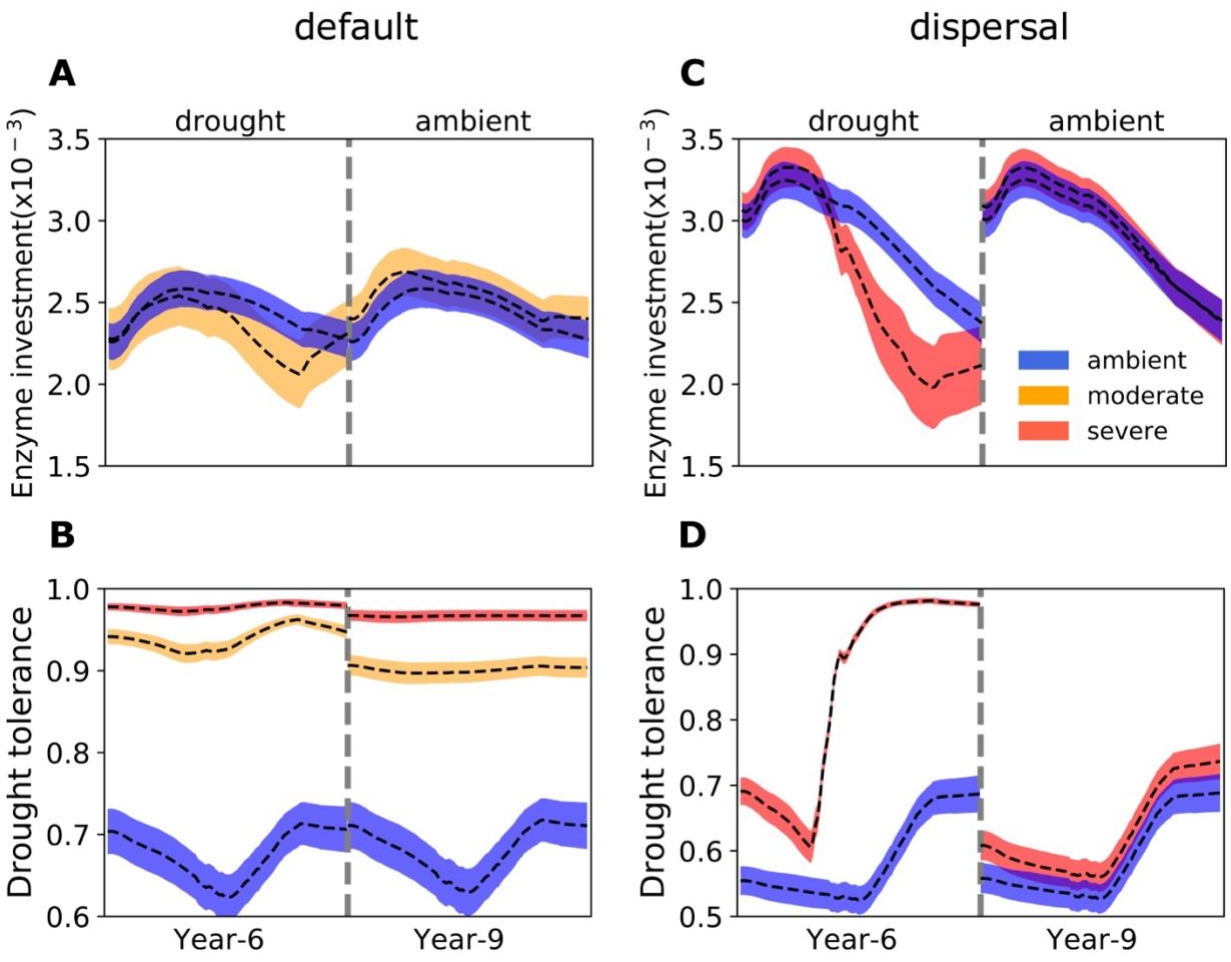

Fig.2 Seasonal dynamics of community-level enzyme investment and drought tolerance of microbial communities under different drought scenarios. (**A, B**) Enzyme investment and drought tolerance during year 6 (3rd year under drought) and year 9 (3rd year after drought) under three scenarios (ambient, moderate, and severe) without dispersal, respectively. (**C, D**) The same for communities with dispersal under two scenarios (ambient and severe). Dashed lines and color bands are means and 95% confidence intervals (n=40).

3.2 Responses to and recoveries from drought disturbance of varying severity

Variation in drought severity altered the microbial community to varying extents (**Fig. 1B, C**). Total biomass declined significantly, with the severe scenario declining the most by about 50%

to a peak less than 10 mg C cm^{-3}. Composition of the communities changed dramatically in terms of taxonomic richness and abundance after 2 years of drought perturbation with differing levels of drought tolerance and enzyme investment. Compared to the ambient scenario, drought tolerance increased significantly across the whole season from as low as only 0.62 to 0.92 of the moderate scenario and to 0.97 of the severe (**Fig. 2A,B**). However, the community enzyme investment only declined significantly in the severe scenario across the dry season and did not change much in the moderate scenario on average besides the later stage in dry season (**Fig. 2A,B**). These trait changes dictated differences in community-level carbon allocation between enzymes and osmolytes and thus yield (**Fig. 3A; Supporting Fig. 5A**). Under the moderate scenario, the percentage of assimilated carbon allocated to osmolytes ranged between 65–85%, compared to the ambient range of 50–70%, whereas enzyme allocation was consistently lower (10% on average) than the ambient (20% on average). However, the resulting yield was basically similar, ranging between 0 - 30%, though a few points in the ambient were higher (reaching at most 40%) early in the drought season. Under the severe scenario, the percentage of osmolytes became even higher and enzymes even lower, and the community yield approached zero more often. Eventually, these differences in community resource allocation between osmolytes and enzymes were manifested in the dampened degradation of substrates over the grid, with the two drought scenarios resulting in different levels of decomposition declines (average of 57.39 and 85.65%, respectively; **Fig. 4A, B**).

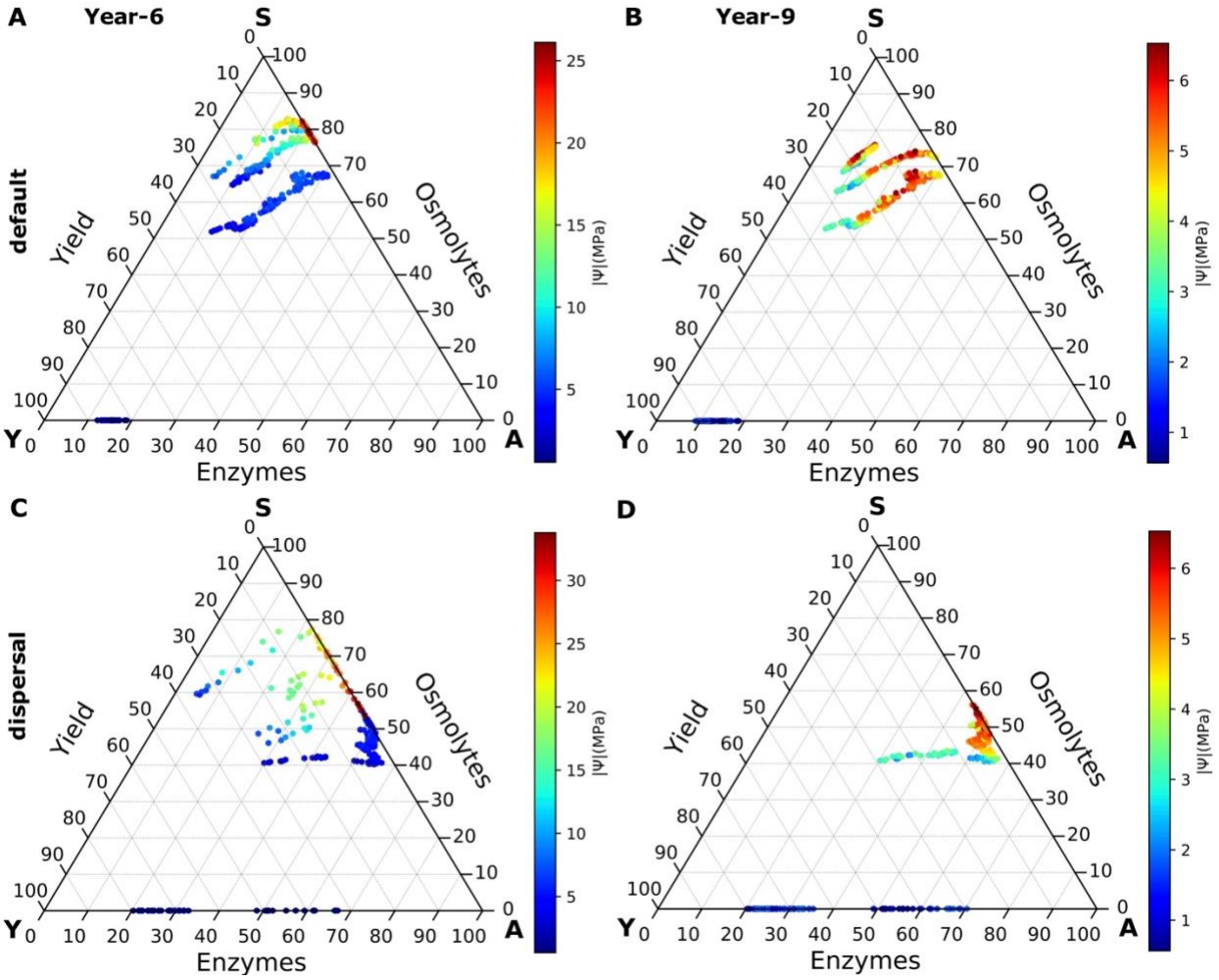

Fig. 3 Ternary plots of community-level allocation of assimilated carbon among enzymes, osmolytes, and yield over time under different drought scenarios. (A, B) Enzyme-Osmolyte-Yield tradeoff of communities during year 6 (3rd year under drought) and year 9 (3rd year after drought), respectively, of the default mode (without dispersal). (**C, D**) The same for the dispersal mode. The Y (Yield), A (Acquisition), and S (Stress) labeled at corners correspond to yield, enzymes, and osmolytes, respectively. See **Supporting Fig. 5** for a version with points differentiated by drought scenario instead of water potential.

Once the ambient conditions were re-imposed, after 2 years (year 9) new stable microbial communities formed (**Fig. 1B, C** and **Supporting Fig. 2C**). Compared to the ambient scenario, these newly-formed communities had different drought tolerance and enzyme investment (**Fig. 2A, B**). Drought tolerance was significantly higher under both the moderate (0.90) and severe scenario (0.96) than under the ambient, though both became a little lower than the communities realized under drought disturbance. In contrast, enzyme investment under the moderate scenario became similar to the ambient community, with only the severe scenario community remaining significantly different. Only the severe community showed a clearly lower allocation to enzymes than the ambient community across the dry season (**Fig. 3B; Supporting Fig. 5B**). This loss of differences in enzyme investment in the moderate community eventually resulted in only the severe scenario displaying significantly reduced degradation compared to the ambient scenario (by 47.72% on average; **Fig. 4B**), although the magnitude of decline was dampened compared to the antecedent drought period because of the relief of drought pressure (**Fig. 4A**). It is noteworthy that prior to year 9, the degradation changes resulting from the transient communities (year 7) were significant for both drought scenarios (an average decline by 18.00 and 55.52%, respectively).

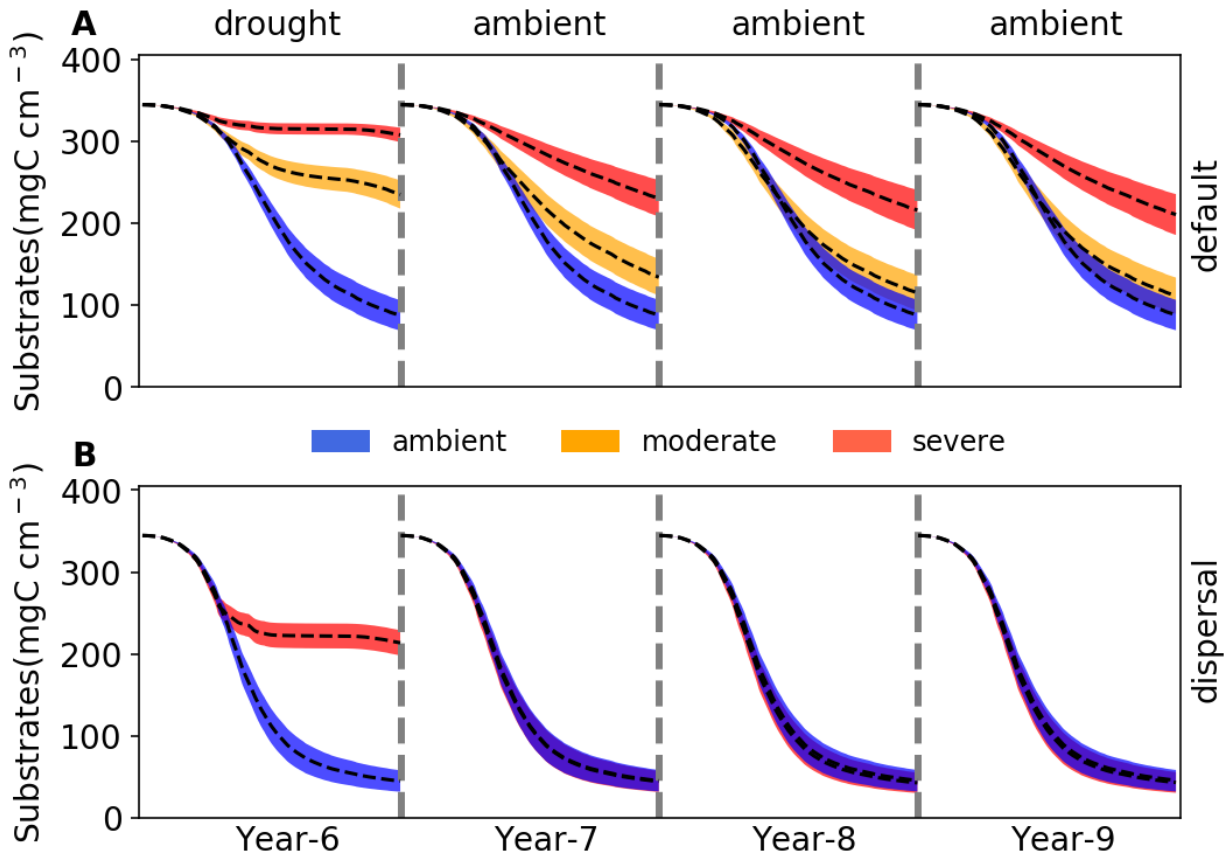

Fig. 4 Changes in substrates driven by drought. (**A**) Total substrates on the spatial grid over year 6-9 under three different scenarios (ambient, moderate, and severe) without dispersal. (**B**) The same for simulations with dispersal under ambient and severe scenarios. Dashed lines and colored bands are means and 95% confidence intervals (n = 40), respectively. See **Supporting Fig. 6** for an example illustration of the underlying substrate-specific changes.

3.3 Responses to and recoveries from the severe drought disturbance with dispersal

With dispersal of taxa from the same microbial pool at the beginning of each year, the overall responses to the severe drought disturbance were similar to the default mode, though with differing magnitudes and seasonal patterns. With dispersal the microbial community also saw both lower total biomass and declined taxonomic abundance, particularly significant during the dry

season, but remained higher than the default mode (**Fig. 1E**). This stable community realized had significantly different community enzyme investment and drought tolerance from the ambient as well but with a different seasonal pattern compared to the default mode. The enzyme investment sharply declined from a peak of 0.0033 to 0.0020, and the drought tolerance increased sharply from 0.60 to 0.97 across the dry season, increasing their differences from the ambient over time (**Fig. 2C,D**). These changes resulted in the community allocating more assimilated carbon to produce osmolytes and less to enzymes, which resulted in zero yield when drought was most severe during the dry season (**Fig. 3C; Supporting Fig. 5C**). All these changes pointed to significant declines in decomposition of substrates (**Fig. 4C**; an average decline of 56.29% that was lower than the default mode)

However, when ambient conditions were re-imposed, recovery from drought was rapid compared to the default mode. After 2 years, the community became similar to the ambient (**Fig. 1E**), a stark contrast to the default mode (**Fig. 1C**). This compositional similarity coincided with similar community enzyme investment (**Fig. 2C**) and drought tolerance (**Fig. 2D**), which resulted in the same community-level allocation of assimilated carbon among enzymes (30 - 60%), osmolytes (40 - 60%), and thus yield (0 – 30%; **Fig. 3D; Supporting Fig. 5D**). These similarities eventually had the almost completely same substrates' decomposition (**Fig. 4D**). In fact, in contrast to the default mode, the transient community did not show significant effects since the very 1st year after drought (year 7; **Fig. 4D**). This was attributed to the fact that the community became same immediately after the drought. This was also why the moderate scenario in dispersal mode was omitted, as there was no legacy even under the severe scenario.

4 Discussion

With trait-based modelling in a mechanistically explicit fashion, this study examined the relationships between drought legacy and drought severity and dispersal in simulated litter microbiomes. Manifestation of drought legacy at the system level in terms of litter decomposition was contingent on drought severity and microbial dispersal, forming an array from persistent through transient to no legacy at all (**Fig. 4**). Such a set of representative legacy scenarios with respect to property, magnitude, and duration point to a more overarching mechanistic basis underpinning drought legacy in soil microbiome—tradeoff between enzyme and drought tolerance.

Transient legacy under moderate drought

Clearly, the severity of drought disturbance matters in the magnitude and duration of legacy formed via determining the extent to which a microbial community can adapt (**Fig. 4A**). By increasing the drought intensity we revealed legacies from transient to persistent. It is easy to expect no legacy at all if with an even weaker disturbance, which we did not cover in the current study. In addition, the drought disturbance was all lasted long enough to enable communities reach a stable state. These simulations in regard to intensity and duration of the drought disturbance were only a sample of the broad spectrum of actual drought disturbance in terms of frequency, intensity, and duration and were implemented with in mind to uncover and demonstrate the underlying mechanisms.

Drought disturbance of a relatively low severity, though being able to result in a declined decomposition after disturbance conferred by the transient community, eventually saw a disappearance of the legacy effect (**Fig. 4A**), which we dub transient legacy. This transient legacy matches very well the field rainfall manipulative experiment with a reciprocal design at the same

site as this modelling study, which observed mitigated drought legacy in terms of litter decomposition within three years (**Martiny et al. 2017**). It is noteworthy that this transient legacy arose from an eventual stable community with the same functioning but different composition and biomass. However, with a total biomass difference as large as 50% (peak biomass under the moderate scenario, but a similar total biomass at the end; **Fig. 1B**), the role of biomass difference can be largely excluded in this eventual functional indifference. This exclusion of biomass change in contributing to legacy formation is consistent with findings from both a field manipulative experiment at Loma Ridge, Southern California (**Martiny et al. 2017**) and a reciprocal transplant study across a climate gradient in Southern California (**Glassman et al. 2019)**. Rather, the eventual loss of legacy under a relatively less intense drought disturbance fundamentally resulted from the remaining same community enzyme investment (accompanied by a realization of higher community drought tolerance) though compositionally different (**Fig. 2A, B**). Such a compositional but not functional change in the new stable system after a disturbance, which has been widely observed across natural systems (e.g., **Ives & Carpenter 2007; Fukami 2015**), reflects a broad notion of functional similarity in the soil microbiome (**Allison and Martiny 2008**). It is this transient legacy that dictates the resilience of microbial systems and other natural systems when moderately perturbed, underlying which functional redundancy is one key factor for microbial systems in particular (e.g., **Louca et al. 2018**).

Persistent legacy under severe drought

In contrast, persistent legacy (**Fig. 4B**) can be shaped by a stronger drought disturbance that can push the community to reach an even higher drought tolerance by sacrificing more of the capability in enzyme investment (including a loss of drought-intolerant taxa), thereby forming a

community not only compositionally but also functionally different (**Fig. 2A,B**). A similar long-term legacy but expressed in soil heterotrophic respiration was also observed by microcosm and field transplant experiments by **Hawkes et al. (2017)**. More generally, historical contingency of alternative stable system with a functional difference has been widely reported across different systems with disturbances of drought and beyond: e.g., in gut microbiota experiencing transient osmotic perturbation (**Tropini et al. 2018**) and in forest biome across tropical (**Hirota et al. 2011**; **Staver et al. 2011**) and boreal forest (**Herzschuh 2019**), as well as in small pond systems (**Chase 2003**). A persistent legacy means the loss of systems resilience with severe disturbance.

Disappearance of legacy under severe drought b/c dispersal

However, microbial communities, though being able to carry the legacy effects of severe drought disturbance into the future, are faced with other disturbances; therefore, drought legacy may be subject to changes. This study demonstrated that dispersal is one such process that can negate formation of even transient legacy in organic matter decomposition. By constantly introducing taxa from the same microbial pool in each new year, we found that dispersal with even the severe drought disturbance can completely mitigate the physiological tradeoff-mediated drought selection on a microbial community (**Fig. 1E**). As a result of community similarities in drought tolerance and enzyme investment (**Fig. 2C, D; Fig. 3D**), dispersal can overwhelm the drought legacy in organic matter decomposition (**Fig. 4B**). This disappearance of legacy suggests that dispersal can increase microbial systems resilience to drought disturbance (**Allison and Martiny 2008**), forming a stark contrast to the severe drought disturbance without dispersal as discussed above. We must acknowledge that factors in dispersal influencing resident community are manifold (**Vila et al. 2019**); for instance, timing (i.e., priority effects; **Fukami 2015**) and

velocity (**Evans et al. 2019**) both have been suggested to be important. Moreover, even an unsuccessful dispersal with only transient interactions can induce an alternative stable state functioning differently (**Amor et al. 2020**). Therefore, the scenario examined in this study (with a solely purpose of revealing underlying mechanisms) by no means is exclusive. For example, in a field transplant experiment but with passive dispersal **Hawkes et al. (2017)** did not find any apparent mitigation of historical rainfall legacy in soil respiration. Therefore, responding to the huge variation in the dispersal process, a microbial community could instead present compositional and functional changes to varying extents (e.g., **Fukami 2015**) and hence varying magnitudes of legacy in decomposition, which warrant more explorations.

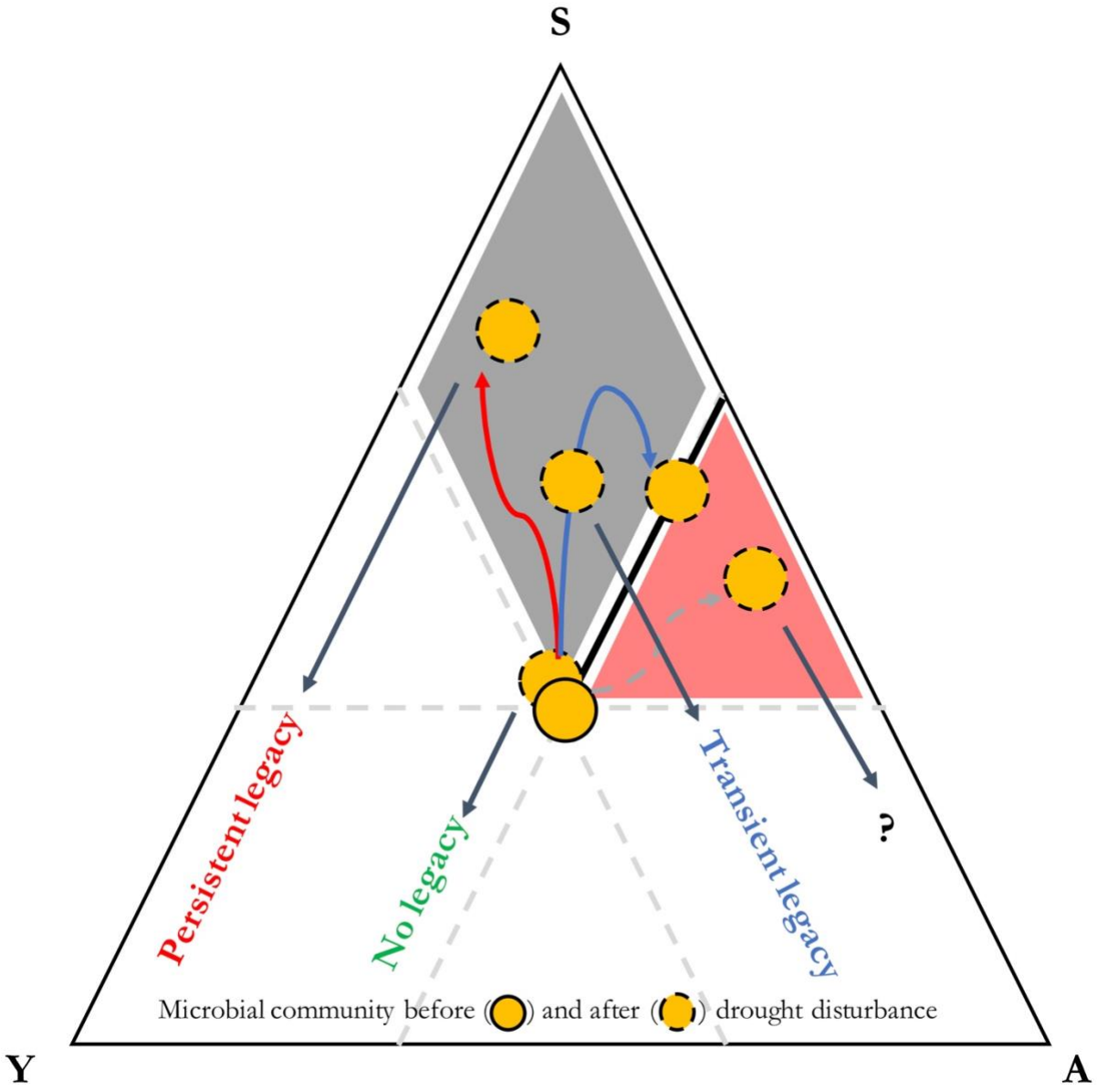

Fig. 5 A coherent mechanistic framework of drought legacy based on YAS. Drought legacy is contingent on the trajectory of a microbial community on the Y-A-S space. There will be no legacy if a community does not move at all or move along the thick black line. Instead, if the community moves into and stays in the grey region, persistent legacy will occur. However, if the community eventually leaves the grey region and settles on the thick black line, only transient legacy can occur. In addition, a speculation of another trajectory is included: a community moving into the red region

409 with both increased drought tolerance and enzyme investment. Note that it is for an illustration
410 purpose only that the starting microbial community (full yellow circle) does not necessarily stay
411 in the center of the space.
412
413 **A coherent mechanistic framework**
414 From the clear contrasts of cases of low vs. high drought severity (transient vs. persistent
415 legacy) and of cases without vs. with dispersal under severe drought disturbance (persistent legacy
416 vs. no legacy), we can arguably deduce that drought legacy in microbiome functioning can
417 originate from physiological tradeoff between enzyme and osmolyte production and is eventually
418 determined by the position that a community can reach on its potential space constrained by
419 enzyme investment, drought tolerance, and yield (i.e., a coherent YAS-based framework illustrated
420 in **Fig. 5**). For instance, when drought forces the community to move to a position of higher
421 drought tolerance but eventually similar enzyme investment (e.g., low level drought as shown in
422 the moderate scenario; **Fig. 4A**), only transient legacy occurs. However, when a community moves
423 to a position of higher drought tolerance and lower enzyme investment (e.g., under an intense
424 drought as shown in the severe scenario; **Fig. 4A**), persistent legacy in impaired capability in
425 degrading substrates can occur. In contrast, when the community does not move at all on the space
426 (e.g., with dispersal present under even a relatively severe drought; **Fig. 4B**), transient legacy may
427 not be even able to appear.
428 Based on this coherent framework, any agent that is capable of shaping the trajectory of a
429 community on the Y-A-S constrained space may influence the property, magnitude, and/or
430 duration of drought legacy. Mechanisms and factors influencing the tradeoff between enzyme and
431 osmolyte can be complex and manifold. In fact, tradeoffs in microbiome and beyond are complex

in general (e.g., **Berezovsky & Shakhnovich, 2005; Ferenci 2016**); notably, tradeoffs are not necessarily rigid, which may even be the opposite of a tradeoff (e.g., **Tikhonov et al. 2020**). Such complexities can be induced by factors including, among others, drought intensity, dispersal, and potentially many others, as well as processes including, e.g., metabolic plasticity and evolution. For instance, we speculate a fourth legacy scenario of both increased drought tolerance and enzyme investment that emerges from a loss of enzyme-osmolyte tradeoff under certain conditions, which in theory is possible as long as without breaking the constraint of tradeoff with yield (**Fig. 5**). Therefore, broadening the scope of scenarios examined in this study (as discussed earlier on drought disturbance and dispersal) and relaxing assumptions in DEMENTpy offer natural directions in which our study can be extended for enriching the tradeoff-mediated mechanisms underpinning drought legacy.

Implications

In summary, this study revealed a coherent tradeoff-mediated mechanistic framework that can explain a variety of representative drought legacy scenarios in soil microbiome emerging from trait-based microbial community shifts. These mechanistic insights bear immediate implications for understanding soil microbiome organization and resilience and broad consequences for quantifying ecosystems' responses and feedbacks to increasing frequency and severity of drought and other environmental changes. Through cell metabolic plasticity of resource allocation to enzyme versus osmolyte microbial communities achieve self-organization after drought disturbances to reach different states. This drought-based notion can be totally extended to any other disturbances that soil microbiome faces. Thereby, this insight arguably points to next step efforts of leveraging rich -omics information, especially transcriptomics, to better inform such

plasticity expressed in physiological traits at single cell level (e.g., **Hatzenpichler et al. 2020**). An accurate quantification of drought legacy with respect to magnitude and duration would enable a better evaluation of implications of litter decomposition for ecosystem dynamics and functioning. For instance, even a transient legacy of impaired decomposition may enhance carbon sequestration in soil systems at certain temporal scales, but may also allow fuels to accumulate for the next fire season, thereby increasing fire risk (e.g., **Pellegrini et al. 2017**). Additionally, impaired decomposition can inhibit release of nutrients from detritus and thus their return to plants, influencing plant-microbe interactions (e.g., **Legay et al. 2018**). All these and potentially many other cascading changes arising from microbiome legacy would engender more complex feedbacks in ecosystems. Evaluating their implications entails an integrative, holistic view of components in systems across ecosystem and the Earth System scales. To proceed, this study clearly indicates that to really establish a predictive science of ecosystems in the context of projected global climate change, considering history as an essential component means that dimensions and spaces of essential tradeoffs distilled from tremendous taxonomic diversity should be incorporated. This trait-based modelling of soil microbiome, together with progress in trait-based insights into vegetation dynamics, offer an inspirational starting point for moving forward in this direction.

References

Allison, S. D. (2012). A trait-based approach for modelling microbial litter decomposition. Ecology letters, 15, 1058-1070.

Allison, S. D., Lu, Y., Weihe, C., Goulden, M. L., Martiny, A. C., Treseder, K. K., & Martiny, J. B. (2013). Microbial abundance and composition influence litter decomposition response to environmental change. Ecology, 94, 714-725.

Berdugo, M., Delgado-Baquerizo, M., Soliveres, S., Hernández-Clemente, R., Zhao, Y., Gaitán, J. J., ... & Rillig, M. C. (2020). Global ecosystem thresholds driven by aridity. Science, 367, 787-790.

Berezovsky, I. N., & Shakhnovich, E. I. (2005). Physics and evolution of thermophilic adaptation. Proceedings of the National Academy of Sciences, 102, 12742-12747.

Birch, H. F. 1958. The effect of soil drying on humus decomposition and nitrogen availability. Plant and Soil, 10, 9–31.

Borsa, A. A., Agnew, D. C., & Cayan, D. R. (2014). Ongoing drought-induced uplift in the western United States. Science, 345, 1587-1590.

Conradi, T., Van Meerbeek, K., Ordonez, A., & Svenning, J. C. (2020). Biogeographic historical legacies in the net primary productivity of Northern Hemisphere forests. Ecology Letters. https://doi.org/10.1111/ele.13481

Csonka, L. N. (1989). Physiological and genetic responses of bacteria to osmotic stress. Microbiological Reviews, 53, 121-147.

Cuddington, K. (2011). Legacy Effects: The Persistent Impact of Ecological Interactions. Biological Theory, 6, 203–210.

Evans, S.E., Wallenstein, M.D. (2012) Soil microbial community response to drying and rewetting stress: does historical precipitation regime matter? Biogeochemistry, 109**,** 101–116.

Falkowski, P. G., Fenchel, T., & Delong, E. F. (2008). The microbial engines that drive Earth's biogeochemical cycles. Science, 320, 1034-1039.

Ferenci, T. (2016). Trade-off mechanisms shaping the diversity of bacteria. Trends in Microbiology, 24, 209-223.

Gommers, P. J. F., Van Schie, B. J., Van Dijken, J. P., & Kuenen, J. G. (1988). Biochemical limits to microbial growth yields: an analysis of mixed substrate utilization. Biotechnology and Bioengineering, **32**, 86-94.

Green, J.K., Seneviratne, S.I., Berg, A.M. *et al.* (2019). Large influence of soil moisture on long-term terrestrial carbon uptake. Nature, 565**,** 476–479.

Herzschuh, U. (2020). Legacy of the Last Glacial on the present-day distribution of deciduous versus evergreen boreal forests. Global Ecology and Biogeography, 29, 198-206

523 Hinojosa, M. B., Laudicina, V. A., Parra, A., Albert-Belda, E., & Moreno, J. M. (2019). Drought
524 and its legacy modulate the post-fire recovery of soil functionality and microbial community
525 structure in a Mediterranean shrubland. Global Change Biology, 25, 1409-1427.
526
527 Hobbie, J. E., & Hobbie, E. A. (2013). Microbes in nature are limited by carbon and energy: the
528 starving-survival lifestyle in soil and consequences for estimating microbial rates. Frontiers in
529 Microbiology, 4, 324.
530
531 Johnstone, J. F., Allen, C. D., Franklin, J. F., Frelich, L. E., Harvey, B. J., Higuera, P. E., ... &
532 Schoennagel, T. (2016). Changing disturbance regimes, ecological memory, and forest resilience.
533 Frontiers in Ecology and the Environment, 14, 369-378.
534
535 Karhu, K., Auffret, M., Dungait, J. *et al.* (2014) Temperature sensitivity of soil respiration rates
536 enhanced by microbial community response. Nature, 513, 81–84
537
538 Louca, S., Polz, M.F., Mazel, F. et al. Function and functional redundancy in microbial systems.
539 Nat Ecol Evol 2, 936–943 (2018). https://doi.org/10.1038/s41559-018-0519-1
540
541 Manzoni, S., Schimel, J. P., & Porporato, A. (2012). Responses of soil microbial communities to
542 water stress: results from a meta-analysis. Ecology, 93, 930-938.
543
544 McGill, B. J., Enquist, B. J., Weiher, E., & Westoby, M. (2006). Rebuilding community ecology
545 from functional traits. Trends in Ecology & Evolution, 21, 178-185.

546 Meisner, A., Rousk, J., & Bååth, E. (2015). Prolonged drought changes the bacterial growth
547 response to rewetting. Soil Biology and Biochemistry, 88, 314-322.
548
549 Sardans, J., & Peñuelas, J. (2010). Soil enzyme activity in a Mediterranean forest after six years
550 of drought. Soil Science Society of America Journal, 74, 838-851.
551
552 Schimel, J., Balser, T. C., & Wallenstein, M. (2007). Microbial stress-response physiology and its
553 implications for ecosystem function. Ecology, 88, 1386-1394.
554
555 Sinsabaugh, R. L., Manzoni, S., Moorhead, D. L., & Richter, A. (2013). Carbon use efficiency of
556 microbial communities: stoichiometry, methodology and modelling. Ecology Letters, 16, 930-939.
557
558 Tiemann, L. K., & Billings, S. A. (2011). Changes in variability of soil moisture alter microbial
559 community C and N resource use. Soil Biology and Biochemistry, 43, 1837-1847.
560
561 Wang, B., & Allison, S. D. (2019). Emergent properties of organic matter decomposition by soil
562 enzymes. Soil Biology and Biochemistry, 136, 107522.
563
564 Wieder, W. R., Allison, S. D., Davidson, E. A., Georgiou, K., Hararuk, O., He, Y., ... & Todd-
565 Brown, K., 2015. Explicitly representing soil microbial processes in Earth system models. Global
566 Biogeochemical Cycles, 29, 1782-1800.
567

Acknowledgements

All data and code underlying the analyses and illustrations in this manuscript are archived at: https://github.com/bioatmosphere/microbiome-drought-legacy. DEMENTpy code is available at https://github.com/bioatmosphere/DEMENTpy.

Supporting Information

Tradeoff-mediated Drought Legacy in Soil Microbiome

Bin Wang, Steven D. Allison

1 DEMENTpy

DEMENTpy, a trait-based explicit microbial systems modelling framework both mechanistically and spatially, is an effort of mechanistically updating (see **Supporting Fig. 1** for conceptual structure) and programmatically restructuring (see **Supporting Fig. 7** for programming structure) DEMENT that was initially developed in 2012 (**Allison 2012**). The source code in Python is archived at https://github.com/bioatmosphere/DEMENTpy. Processes simulated in DEMENTpy are described below.

1.1 Microbial community initialization

With a trait-based approach, a microbial pool comprises a large number of hypothetical taxa in DEMENTpy is created by randomly drawing values from distributions of various microbial and enzymatic traits (**Supporting Table 1**) and assigning them to different taxa. These hypothetical taxa in the microbial pool with differing combinations of trait values are randomly placed on the spatial grid to form a spatially-explicit microbial community. See animations at https://bioatmosphere.github.io/DEMENTpy/ to get an intuitive notion of this spatial feature, and an application of this feature to addressing enzymatic heterogeneity scaling in **Wang and Allison (2019)**. Trait distributions are all assumed to follow uniform distributions, except that for simplicity, some traits are assumed to be constants, and values of some traits are derived from established correlations with other traits. These distributions and assumptions are largely informed by field- and lab-based experimental works (**Allison 2012; Allison and Goulden 2017**).

Four of the major traits determining intra-cellular metabolism of enzyme and osmolyte and thus mass balance are rates of enzyme production (constitutive and inducible) and rates of osmolyte production (constitutive and inducible). On top of these rates, taxon-specific number of genes encoding different enzymes and osmolytes are determined randomly under the constraint of systems setup. Therefore, rate and number together determine amounts of enzyme and osmolyte a cell can produce. The rate of production of inducible osmolyte is then normalized to a value from 0 to 1, which is regarded as drought tolerance. Such a treatment of drought tolerance is an update to the previous version which instead directly introduced a drought tolerance parameter and imposed a penalty on carbon use efficiency accordingly (**Allison and Goulden 2017**). Starting from osmolyte production to determine drought tolerance is supposed to be more biologically realistic (**Schimel 2007**). Additionally, a whole set of enzymatic traits including Vmax and Km of both enzyme and transporter is employed to explicitly parameterize a certain number of different enzymes and transporters allowed in a system.

1.2 Metabolic production of enzyme and osmolyte

Different individuals (hypothetical taxa) comprising the microbial community complete their demographic processes of growth, mortality, and reproduction while degrading substrates and ingesting monomers under the influence of temperature and water potential. From these underlying processes emerges dynamics and functioning at both the microbial cell level and the whole system level.

Degradation of substrates are calculated explicitly by using different enzymes with different kinetic properties. One principle during the simulation is that every substrate at least has one enzyme to degrade and vice versa. Different monomers are calculated explicitly by having differing transporters to target them. Transporters of different types and amounts are taxon-specific,

which is described immediately below. The governing equation of both substrates' degradation and monomers' uptake follows the Michaelis-Menten equation, which is further constrained by temperature (accounting for temperature impacts on enzymatic kinetics) and water potential (accounting for enzymatic kinetics and diffusion declines arising from drought; **Allison and Goulden 2017**):

$$V = \frac{V_{max} f(T)[S][E]}{K_m + [S]} f(\psi)$$

$$f(T) = e^{\left(-\frac{\boldsymbol{\varepsilon}}{R}\left(\frac{1}{T} - \frac{1}{T_{ref}}\right)\right)}$$

$$f(\psi) = e^{k\psi}$$

where *E* and *S* represent enzyme and substrate concentration, respectively, *Vmax* represents the enzyme catalytic constant, K_m denotes the concentration of *S* at which *V* is one half V_{max}, $\boldsymbol{\varepsilon}$ is enzymatic activation energy, *R* is universal gas constant, and *k* is a coefficient controlling water potential sensitivity that distinguishes between degradation and uptake.

Intra-cellular production of enzymes and osmolytes are described below in detail with respect to simulation methods and their underlying rationales. Cellular metabolism explicitly deals with both the carbon upon uptake from degraded substrates and the carbon in biomass of microbial cells inducibly and constitutively (**Supporting Fig. 3**). The metabolic processing of assimilated carbon after growth respiration (constrained by a constant) is directed to enzyme (and respiration) and osmolyte production (and respiration; **Csonka 1989; Witteveen and Visser 1995**), which are treated horizontally in the model without prescribing an order. The carbon left after these processes accumulates toward biomass. We assume the constitutive osmolyte production rate (*Osmo_Con*) varies across taxa without depending on water potential, accounting for bacterial/fungal cell's allocation of biomass to keep a water potential balance across cell wall (**Csonka 1989**). In contrast,

taxon-specific inducible production of osmolytes (O_{ind}) is subject to constraints from water potential and is calculated following:

$$O_{ind}(\mathrm{i}) = \begin{cases} O_{ind}(i), & \psi \geq \psi_{th} \\ O_{ind}(i)\ (1\ -\ \alpha\psi), & \psi < \psi_{th} \end{cases}$$

where O_{ind}, indexed by taxon i, is the i_{th} taxon's inducible osmolyte production rate, ψ is the daily water potential, α is a water potential coefficient , and ψ_{th} is a system water potential constant, below which inducible osmolyte production is activated. Though with a differing production rate across taxa, osmolyte in the current version (without further differentiating among different osmolytic compounds) is assumed to hold a constant stoichiometry of C/N = 3, which governs consumption of N in intracellular metabolism. This ratio is based on an average of the three most common osmotic compounds in bacteria (**Csonka 1989**): proline ($C_5H_9NO_2$), glycine betaine ($C_5H_{11}NO_2$), and glutamine ($C_5H_{10}N_2O_3$).

Arising from metabolic production of enzyme and osmolyte, mortality of microbial cells is simulated both deterministically by accounting for mass balance relative to a threshold and stochastically based on death probability constrained by drought tolerance and water potential. Here the taxon-specific mortality probability (*Mort*) is calculated following:

$$Mort_i = Death\_basal_i[1 - Death\_rate_i(1 - Tol_i)(\psi - \psi_{th})\ ]$$

where *Death_basal*, indexed by *i*, is the i_{th} taxon's basal mortality probability, *Death_rate* is a death probability coefficient controlling water potential sensitivity, *Tol* is i_{th} taxon's drought tolerance, and ψ_{th} is a system water potential constant. Microbial cells that are either out of mass

balance or randomly killed are designated as dead ones, removed from the microbial community, and added into the substrates pools as dead microbes. Microbial reproduction is simply calculated by splitting microbes into two halves, which disperse to surrounding grid boxes on the spatial grid.

2. Calculation of community-level traits

Community-level enzyme investment (E_{com}) and drought tolerance (D_{com}) weighted by biomass are calculated as:

$$E_{com} = \sum_{i}^{n} EiMi$$

$$D_{com} = \sum_{i}^{n} DiMi$$

respectively, where *Ei* and *Di* refer to the i_{th} taxon's enzyme production rate and drought tolerance, respectively, and *Mi* is the relative biomass of the i_{th} taxon in the community.

References

Allison, S. D. (2012). A trait-based approach for modelling microbial litter decomposition. Ecology letters, 15, 1058-1070.

Allison, S. D., & Goulden, M. L. (2017). Consequences of drought tolerance traits for microbial decomposition in the DEMENT model. Soil Biology and Biochemistry, 107, 104-113.

Bugmann, H., Fischlin, A., & Kienast, F. (1996). Model convergence and state variable update in forest gap models. Ecological Modelling, 89, 197-208.

Wang, B., & Allison, S. D. (2019). Emergent properties of organic matter decomposition by soil enzymes. Soil Biology and Biochemistry, 136, 107522.

Supporting Table 1 Major microbial and enzyme parameters and their values

Parameter	Value	Unit	Note
max_size_b	2	mg cm-3	C quota threshold for bacterial cell division
Cfrac_b	0.825	mg mg-1	Bacterial C fraction
Nfrac_b	0.16	mg mg-1	Bacterial N fraction
Pfrac_b	0.015	mg mg-1	Bacterial P fraction
Crange	0.09	mg mg-1	Tolerance on C fraction
Nrange	0.04	mg mg-1	Tolerance on N fraction
Prange	0.005	mg mg-1	Tolerance on P fraction
C_min	0.086	mg cm-3	threshold C concentration for cell death
N_min	0.012	mg cm-3	threshold P concentration for cell death
P_min	0.002	mg cm-3	threshold C concentration for cell death
Uptake_C_cost_min	0.01	transporter mg-1 biomass C	Minimun per enzyme C cost as a fraction of uptake
Uptake_C_cost_max	0.1	transporter mg-1 biomass C	Maximum per enzyme C cost as a fraction of uptake
Uptake_Maint_cost	0.01	mg C transporter-1 day-1	Respiration cost of uptake transporters
Enz_per_taxon_min	0		Minimum number of enzymes a taxon can produce
Enz_per_taxon_max	40		Maximum number of enzymes a taxon can produce
Enz_Prod_min	0.00001	mg C mg-1 day-1	Minimum per enzyme production cost as a fraction of C uptake rate
Enz_Prod_max	0.0001	mg C mg-1 day-1	Maximum per enzyme producton cost as a fraction of C uptakte rate
Constit_Prod_min	0.00001	mg C mg-1 day-1	Minimum per enzyme production cost as a fraction of biomass C
Constit_Prod_max	0.0001	mg C mg-1 day-1	Maximum per enzyme production cost as a fraction of biomass C
Osmo_per_taxon_min	1		Minimum number of osmolyte a taxon can produce
Osmo_per_taxon_max	1		Maximum number of osmolyte a taxon can produce
Osmo_Consti_Prod_min	0.0000001	mg C mg-1 day-1	Minimum per osmolyte production cost as a fraction of biomass C
Osmo_Consti_Prod_max	0.000001	mg C mg-1 day-1	Maximum per osmolyte production cost as a fraction of biomass C
Osmo_Induci_Prod_min	0.01	mg C mg-1 day-1	Minimum per osmolyte production cost as a fraction of C uptake rate
Osmo_Induci_Prod_max	0.1	mg C mg-1 day-1	Maximum per osmolyte production cost as a fraction of C uptake rate
CUE_ref	0.5	mg mg-1	Growth efficiency at the reference temperature
CUE_temp	-0.005	mg mg-1	Growth efficiency change with enzyme investment
death_rate_bac	0.001		Bacterial death rate
basal_bac	10		Bacterial basal death probability
wp_th	-2		water potential threshold at which osmolyte is induced
alpha	0.01		Osmolyte production change with water potential
Vmax0_min	5	mg substrate mg-1 enzyme day-1	Minimum Vmax for enzyme
Vmax0_max	50	mg substrate mg-1 enzyme day-1	Maximum Vmax for enzyme

Uptake_Vmax0_min	1	mg substrate mg-1 substrate day-1	Minimum uptake Vmax
Uptake_Vmax0_max	10	mg substrate mg-1 substrate day-1	Maximum uptake Vmax
Uptake_Ea_min	35	kj mol-1	Minimum activation energy for uptake
Uptake_Ea_max	35	kj mol-1	Maximum activation energy for uptake
Km_min	0.01	mg cm-3	Minimum Km
Uptake_Km_min	0.001	mg cm-3	Minimum uptake Km
Vmax_Km	1	mg enzyme day cm-3	Slope for Km-Vmax relationship
Vmax_Km_int	0	mg cm-3	Intercept for Km-Vmax relationship
Uptake_Vmax_Km	0.2	mg biomass day cm-3	Slope for uptake Km-Vmax relationship
Uptake_Vmax_Km_int	0	mg cm-3	Intercept for uptake Km-Vmax relationship
Specif_factor	1		Efficiency-specificity

117

Supporting Table 2 Substrate concentrations initialized in DEMENT simulations (mg cm^{-3}).

Substrate	C	N	P
DeadMic	0	0	0
DeadEnz	0	0	0
Cellulose	146.89	0	0
Hemicellulose	85.855	0	0
Starch	12.21	0	0
Chitin	4.9952	0.83254	0
Lignin	48.51	0.40425	0
Protein1	10.6	2.09704	0
Protein2	10.6	2.09704	0
Protein3	10.6	2.09704	0
OrgP1	12.48	0	0.478469
OrgP2	1.8182	0.79745	0.478469

118

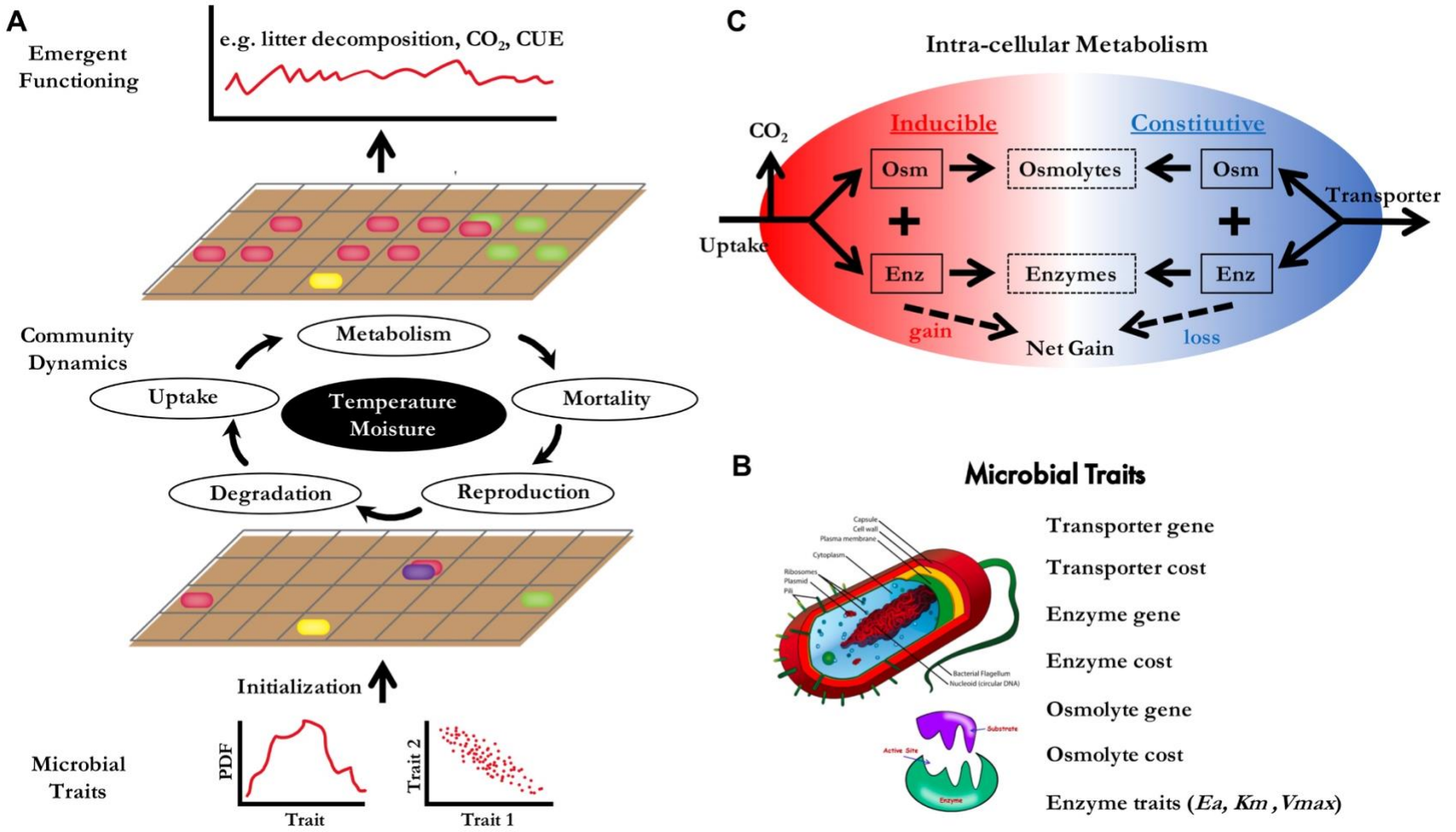

Supporting Fig. 1 DEMENTpy conceptual structure and underpinning traits and intra-cellular metabolism.

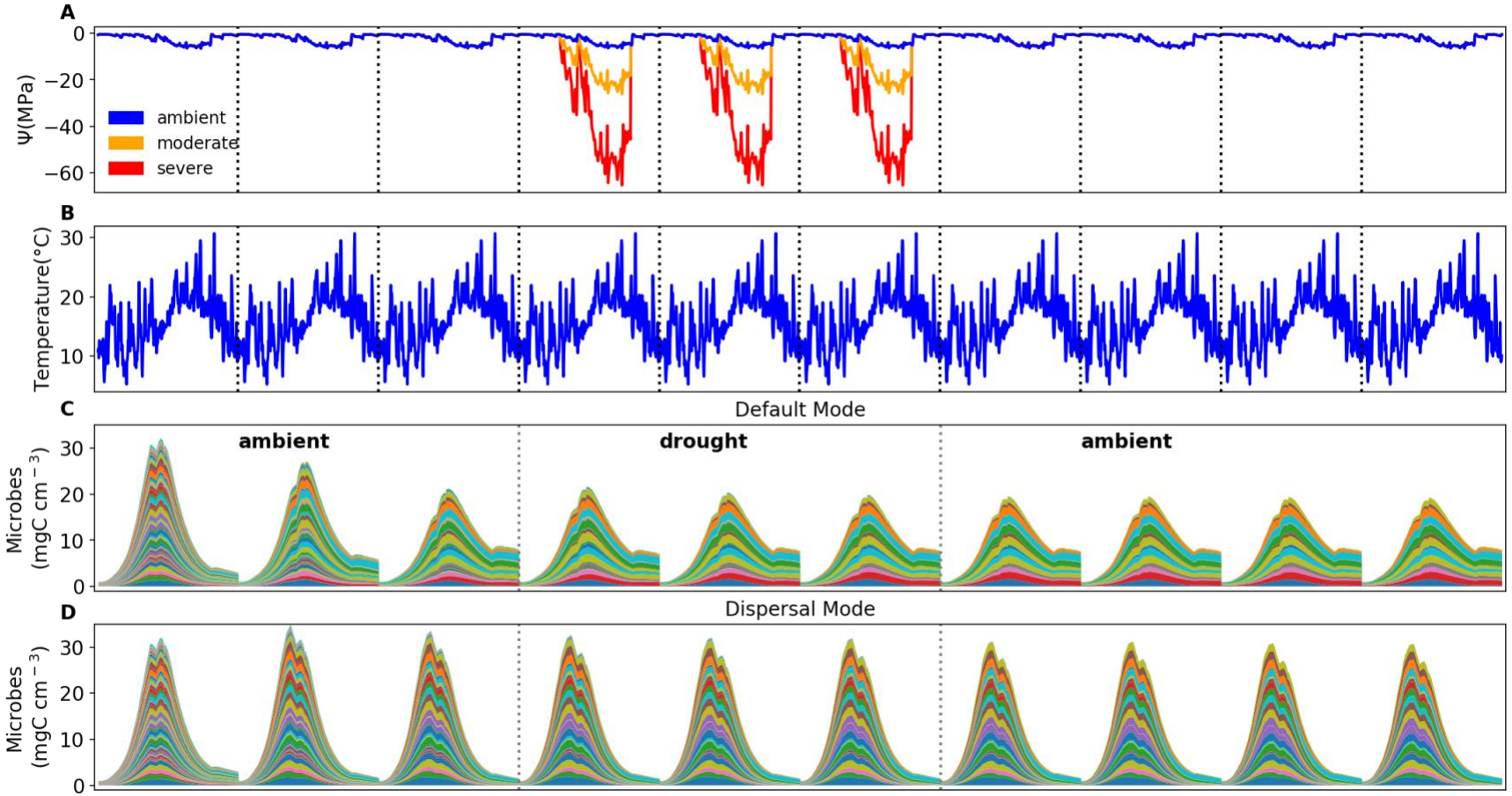

Supporting Fig. 2 Environmental forcing and microbial community dynamics. (**A**) Ambient daily water potential of 2011, with the orange and red line denoting the moderate and severe drought scenario, respectively, which are manipulated values simply by multiplying the water potential across the dry season (from April through September) by 4 and 10, respectively. (**B**) The corresponding daily temperature. (**C, D**) Microbial community dynamics of the default vs. dispersal mode over 10 years under the ambient drought

scenario. The simulation experiences three phases as separated by the dashed grey lines: a spin-up phase of three years to realize a relatively stable community; a disturbance phase of imposing different drought scenarios for three years; and a final recovery phase after drought disturbance. Colored bands represent different hypothetical taxa.

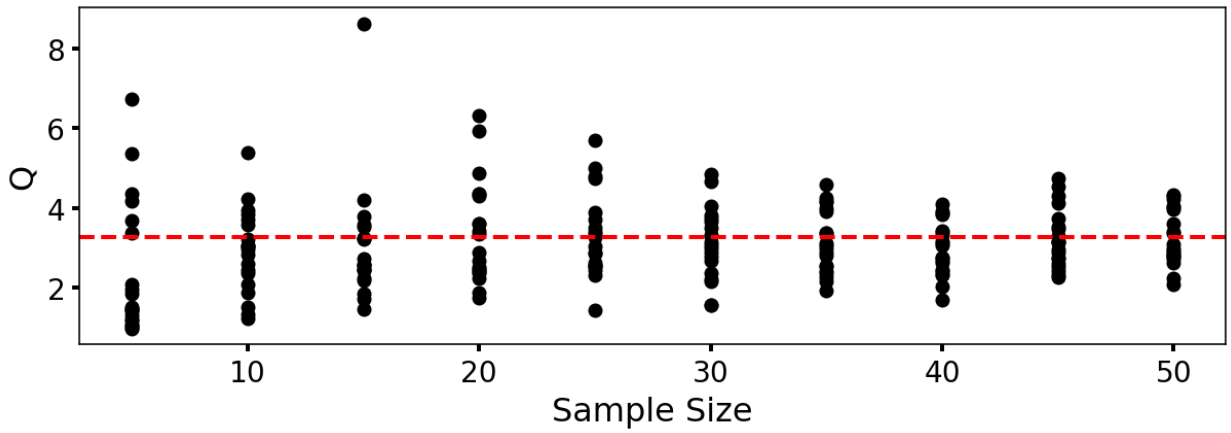

Supporting Fig. 3 DEMENTpy (v1.0) stochasticity convergence analysis. Q (quotient) is calculated as (90% percentile -10% percentile)/median with the data of degradation of substrates following Bugmann et al. (1996). Each sample size has 20 replicates that were randomly drawn from a sample pool of 112 runs. This analysis illustrates that a sample size of 40, which starts displaying relatively stabilized and converged variation, may be an appropriate choice considering a tradeoff of reliability vs. consumption of computing resource.

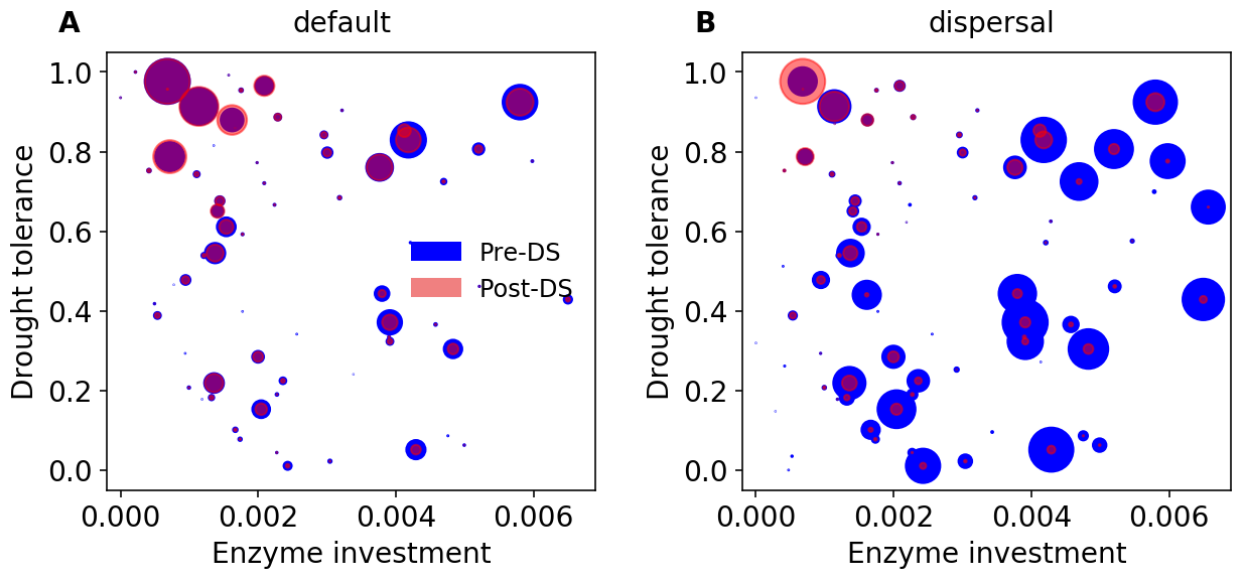

136

137 **Supporting Fig. 4 Taxonomic changes in traits across dry season. (A)** Taxon-specific traits of

138 drought tolerance and enzyme investment of a microbial community without dispersal before (blue)

139 and after the dry season (red) under the ambient scenario. (**B**) The same for a microbial community

140 with dispersal. Each point corresponds to a different taxon, and the size is proportional to its

141 biomass.

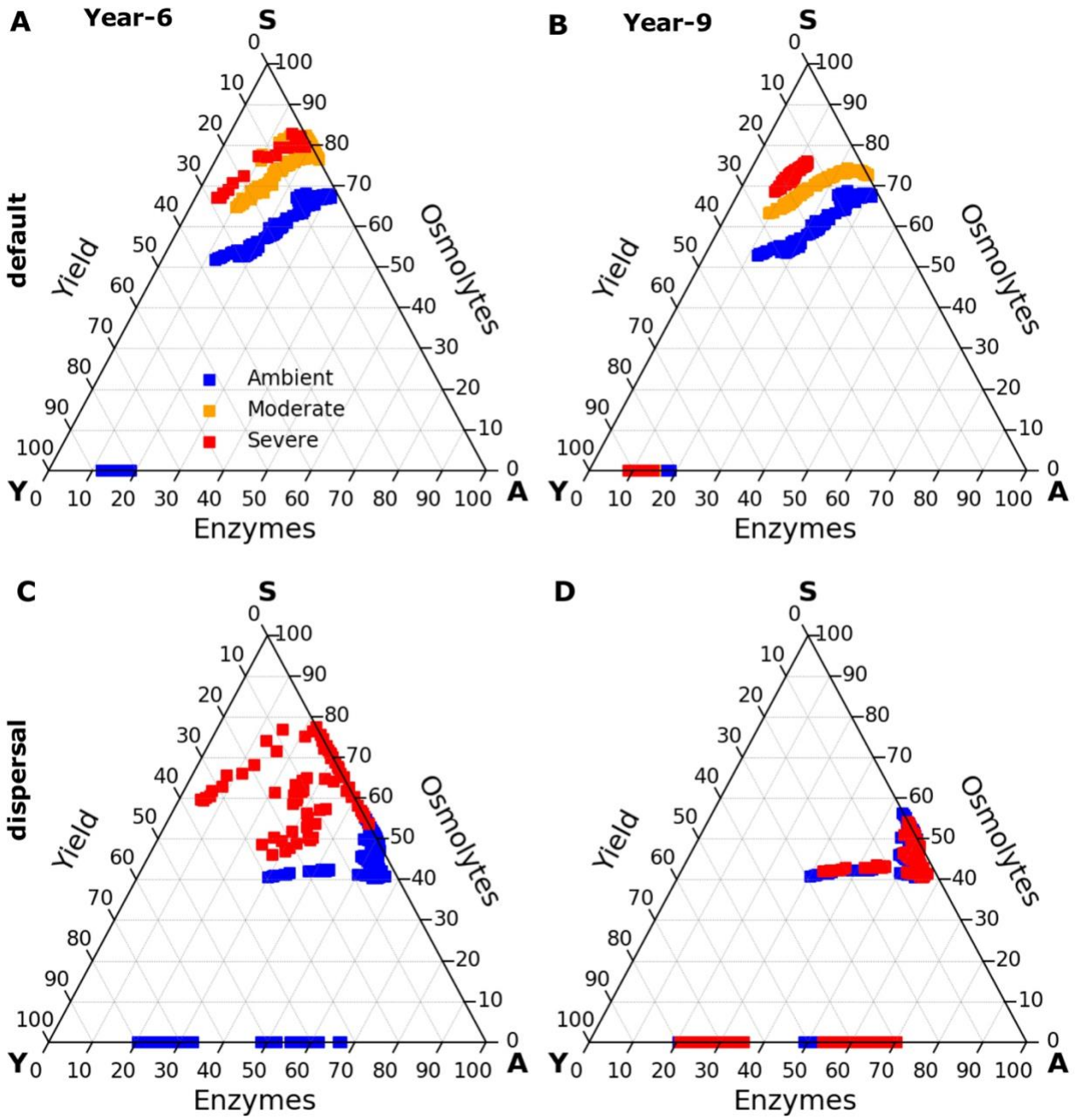

142

143 **Supporting Fig. 5 Ternary plots of community-level allocation of assimilated carbon among**

144 **enzymes, osmolytes, and yield over time under different drought scenarios. (A, B**) Enzyme-

145 Osmolyte-Yield tradeoff of communities during year 6 (3rd year under drought) and year 9 (3rd

146 year after drought), respectively, of the default mode (without dispersal). (**C, D**) The same for the

dispersal mode. The Y (Yield), A (Acquisition), and S (Stress) labeled at corners correspond to yield, enzymes, and osmolytes, respectively. Points with negative net biomass gain were omitted.

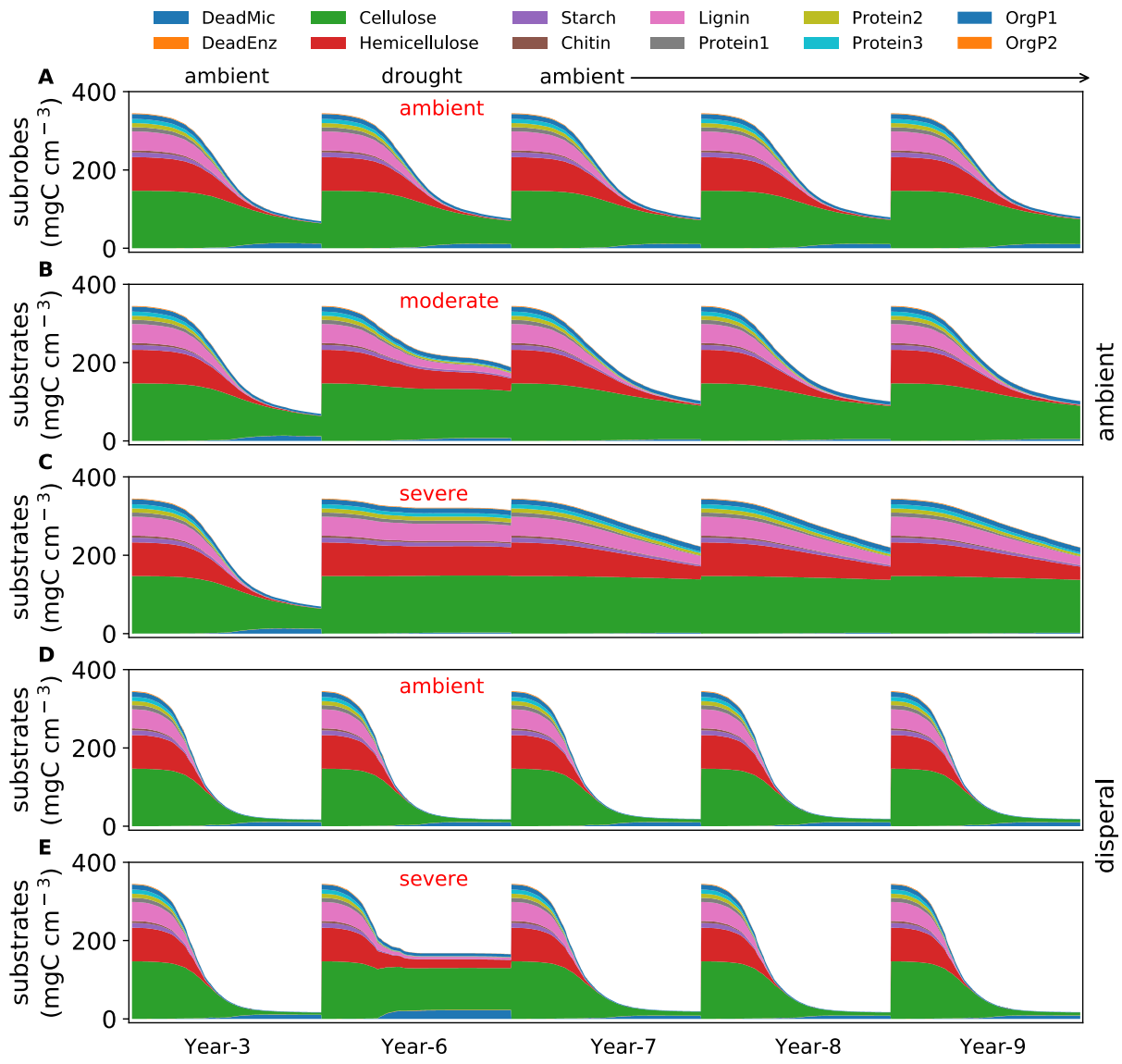

150

151 **Supporting Fig. 6 Substrate-specific dynamics under differing drought scenarios. (A, B, C)**

152 the dynamics under ambient, moderate, and severe scenarios in default mode for year 3 and year

153 6 (the 3rd year under drought disturbance) through year 9. (**D, E**) The same for the dispersal mode

154 but with only ambient and severe scenarios. Each color band represents one type of 12 different

155 substrates.

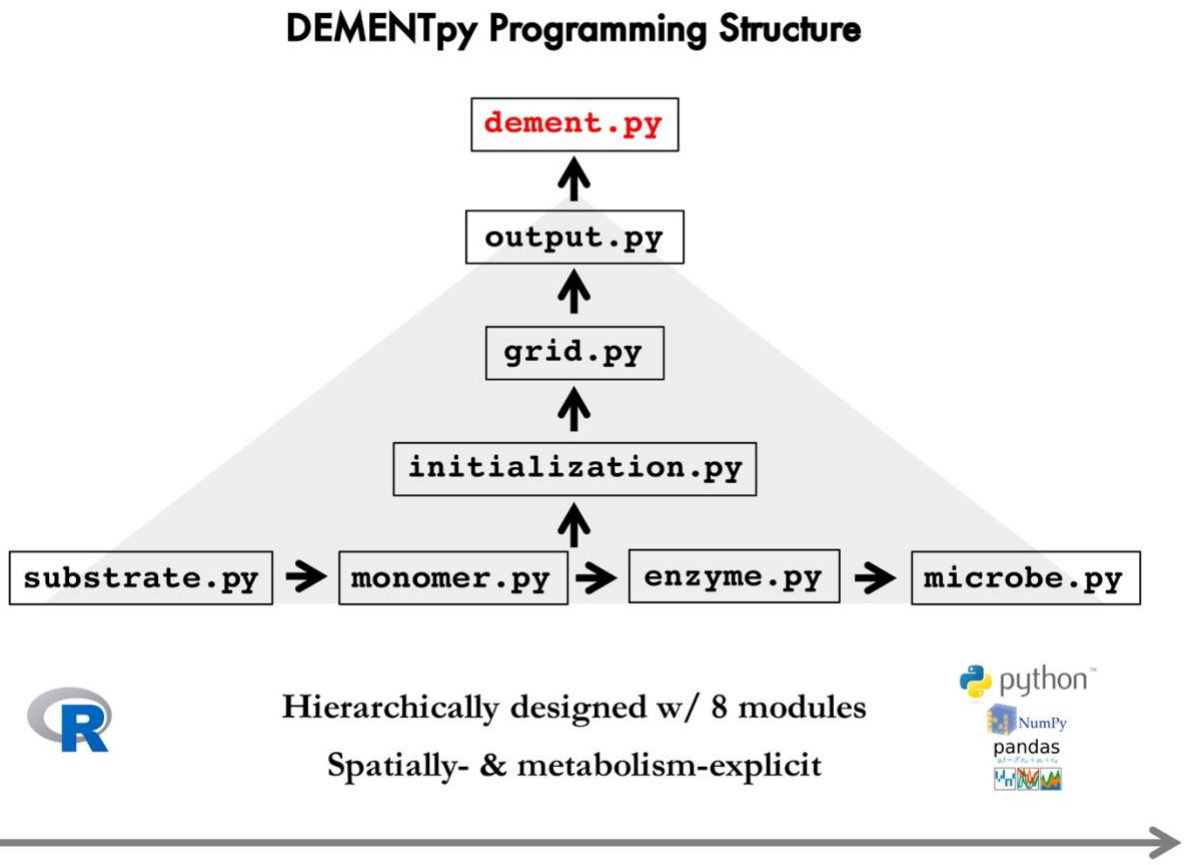

Supporting Fig. 7 DEMENTpy programming structure. DEMENTpy emerges from hierarchically restructuring and mechanistically updating DEMENT programmed in R.